# Diffusion and Convection in Collagen Gels: Implications for Transport in the Tumor Interstitium

Saroja Ramanujan,* Alain Pluen,* Trevor D. McKee,*[†] Edward B. Brown,* Yves Boucher,* and Rakesh K. Jain*

*E. L. Steele Laboratory for Tumor Biology, Department of Radiation Oncology, Massachusetts General Hospital and Harvard Medical School, Boston, Massachusetts 02114; and [†]Biological Engineering Division, Massachusetts Institute of Technology, Cambridge, Massachusetts 02139 USA

ABSTRACT   Diffusion coefficients of tracer molecules in collagen type I gels prepared from 0–4.5% w/v solutions were measured by fluorescence recovery after photobleaching. When adjusted to account for *in vivo* tortuosity, diffusion coefficients in gels matched previous measurements in four human tumor xenografts with equivalent collagen concentrations. In contrast, hyaluronan solutions hindered diffusion to a lesser extent when prepared at concentrations equivalent to those reported in these tumors. Collagen permeability, determined from flow through gels under hydrostatic pressure, was compared with predictions obtained from application of the Brinkman effective medium model to diffusion data. Permeability predictions matched experimental results at low concentrations, but underestimated measured values at high concentrations. Permeability measurements in gels did not match previous measurements in tumors. Visualization of gels by transmission electron microscopy and light microscopy revealed networks of long collagen fibers at lower concentrations along with shorter fibers at high concentrations. Negligible assembly was detected in collagen solutions pregelation. However, diffusion was similarly hindered in pre and postgelation samples. Comparison of diffusion and convection data in these gels and tumors suggests that collagen may obstruct diffusion more than convection in tumors. These findings have significant implications for drug delivery in tumors and for tissue engineering applications.

## INTRODUCTION

Optimal therapy of tumors requires delivery of sufficient amounts of therapeutic agents to the target cancer cells. Thus, the agent must penetrate the tumor interstitial matrix (IM), a complex assembly of collagen, glycosaminoglycans, and proteoglycans (Alberts et al., 1994). Convection through the tumor IM is poor due to interstitial hypertension, leaving diffusion as the major mode of drug transport. As anti-cancer therapy focuses increasingly on larger therapeutics such as liposomes, which are typically at least 90 nm in diameter (Gabizon et al., 1998; Kulkarni et al., 1995), and gene vectors, which range in diameter from 20 to 300 nm (Costantini et al., 2000), diffusion within the tumor IM becomes a greater barrier to delivery (Boucher et al., 1998; Jain, 1999; Netti et al., 1999).

Glycosaminoglycans (GAGs), and particularly hyaluronan (HA), are believed to play a primary but not exclusive role in regulating fluid movement in the IM (Gribbon et al., 1998; Levick, 1987). However, diffusion of large molecules in tumors has been correlated to collagen content and organization, but not to HA content (Netti et al., 2000; Pluen et

al., 2001). These in vivo studies correlated matrix composition to diffusive hindrance, but the biological complexity prohibited detailed analysis of the mechanisms of transport hindrance within the tumor IM. For example, even within a given tumor, Pluen et al. (2001) found varying degrees of collagen organization and heterogeneous distribution of different matrix molecules.

To overcome these problems, we measured diffusion and hydraulic conductivity in pure collagen type I gels and compared these results directly with previously published results for tumors of comparable collagen concentration. Furthermore, we compared the structure of the gels with that seen in tumors. To investigate the role of collagen structure, we compared diffusion in collagen gels and solutions of the same concentrations. The findings presented here are important to the development of improved drug delivery strategies (Jain, 1998) and to pharmaceutical applications of collagen matrices, including the design of tissue substitutes and controlled release devices (Sano et al., 1998).

## MATERIALS AND METHODS

### Experimental techniques

*Preparation of collagen gels*

Vitrogen 100 collagen type I solution was purchased from Collagen Corp. (Cohesion Technologies, Palo Alto, CA) at a concentration of ≈3 mg/ml. The pH and ionic strength were adjusted by addition of NaOH (pH 7.4) and 10× phosphate buffered saline (PBS). To concentrate the solution, the collagen was ultracentrifuged (Beckman LC-300) at 10°C for 26–48 h for preparation of 10–45 mg/ml gels. Supernatant was extracted and pellets were maintained at 4°C. Collagen concentration in the pellet was determined from the difference between precentrifugation and supernatant collagen content as determined by UV spectrophotometry. Pellet concentra-

tion was adjusted by dilution with PBS. The polymerization of highly concentrated collagen solutions leads to the formation of fibers and filaments. To obtain a collagen gel formed predominantly of fibers, 30 ml of neutralized collagen type I (0.4 mg/ml) was polymerized at 32°C for 48 h. The collagen was centrifuged at 11,000 or 25,000 RPM for 12 or 30 min, respectively. The collagen gel was collected on a plastic coverslip that was attached to the bottom of the centrifuge tube. To determine the organization of the fibers and the dimensions of the gel, second harmonic images of the collagen were obtained with a multiphoton microscope (Williams et al., 2001). The collagen concentration estimates were based on the unpolymerized collagen volume and the final gel volume after centrifugation.

For fluorescence recovery after photobleaching (FRAP) experiments at low collagen concentration (2.4 mg/ml), capillary tubes were partially filled with collagen solution and kept for 2 h in a 37°C incubator. After gelation, an aqueous solution of tracer molecules (2 mg/ml) was added to the capillary, which was then sealed and maintained overnight at 37°C to allow tracer penetration of the gel. For FRAP experiments with more concentrated gels, the appropriate tracer molecule solution was added during adjustment of the pellet concentration. The samples were then prepared on concave microscope slides under coverslips and sealed with silicone grease. Samples for permeability and visualization experiments were prepared in Transwell (24 mm diameter; for 0.24% gels) or Snapwell (12 mm diameter, for 1% gels) membrane-bottomed cell culture chambers (Corning Costar Corp., Cambridge, MA) and maintained in a 37°C incubator for at least 1 h to allow gelation. PBS was then added to chambers to maintain hydration.

### Preparation of hyaluronan solutions

Hyaluronic acid sodium salt isolated from rooster comb (Sigma Chemical Co., St. Louis, MO) was dissolved by slow addition of $1\times$ PBS (pH 7.4) for a final concentration of 4 mg/ml. Fluorescent markers at a concentration of 2 mg/ml were added to the solution. The solution was stirred at 4°C for 10 h and subsequently stored at 4°C overnight. Samples were prepared and sealed in capillary tubes as described above for low-concentration collagen gels.

### Measurement of diffusion coefficients

Diffusion coefficients were measured using the FRAP with spatial Fourier analysis technique described previously (Berk et al., 1993, 1997). Briefly, samples permeated with FITC-conjugated tracer molecules were placed on a microscope stage. Each sample was subjected to brief localized 488 nm irradiation from a krypton-argon laser, resulting in bleaching of fluorescence in the irradiated spot (radius $\sim20\ \mu$m). Images were recorded by CCD camera as the bleached spot recovered fluorescence. The diffusion coefficient was extracted from the exponential time decay of the spatial Fourier transform of fluorescence intensity. The diffusion coefficient for a given sample represents the average of 5–10 FRAP measurements in the sample. When not specified otherwise, three gel samples were used to determine the diffusion coefficient of each molecule-gel combination. Tracer molecules including lactalbumin (LA), bovine serum albumin (BSA), and dextrans of molecular weights 4.4 K-2 M were purchased in FITC-labeled form (Sigma). Nonspecific IgG was purchased unlabeled (Sigma) and subsequently conjugated to FITC using the Fluo-EX labeling kit (Molecular Probes, Portland, OR).

Collagen gel samples were prepared as described above and maintained at 37°C throughout diffusion measurements. For measurements in unassembled collagen solutions, samples were maintained at temperatures between 12 and 17°C by supporting the sample on a metal plate in contact with an ice pack. Gelation did not occur at these temperatures, as detected by a lack of OD450 absorbance, indicating no turbidity or light-scattering in these samples. For both gels and solutions, temperature was continuously monitored using a thermocouple and maintained within $\pm$ 1°C for all

measurements on a given sample. Measurements were also made in solutions of HA (Sigma) at pH 7.4 and 37°C.

### Measurement of Darcy permeability

Permeability was measured by monitoring flow rate through collagen gels under hydrostatic pressure in an apparatus described previously (Chang et al., 2000). Briefly, Transwell or Snapwell cell-culture chambers containing gel samples supported on a highly porous membrane were fit snugly into a sample holder and maintained at 37°C. By adjusting the height of the downstream reservoir, a constant hydrostatic pressure was applied to force flow through the gels. The flow was directed through a thin capillary into which one small air-bubble had been injected. Air-bubble motion was visually undetectable due to the low flow rates through the samples. Thus, the linear velocity of the air-bubble was monitored by a photodiode attached to a servo-null motor, which tracked the bubble for 30 min–1 h and was used to determine volumetric flow rates. Hydrostatic pressure ($\Delta P$) of 5–15 cm $H_2O$ (depending on sample concentration) were imposed to create flow that resulted in the lowest measurable bubble velocity. Low concentration (0.24%) gels were not tested, as they were not sufficiently viscous/solid. Gels at 1% were cast in Transwell chambers that fit directly into the apparatus sample holder. Higher concentration gels ($\geq$1%) were cast in Snapwell inserts, and a silicone ring was used to seal the space between the insert and the outer Transwell support. All junctions between plastic and gels (collagen or silicone) were sealed with Krazy Glue to prevent leakage. Leaky samples were quickly detected due to immediate, rapid movement of the air-bubble and were discarded. The surface area ($A$) and thickness ($L$) of each sample were measured. The Darcy permeability ($K$) of the sample was then determined from the time-averaged volumetric flow rate ($Q$) and viscosity ($\mu$) using Darcy's Law:

$$Q = K \frac{A}{L} \frac{\Delta P}{\mu}.$$

Measurement of gel permeability by this method was validated using agarose gels prepared and sealed in identical holders. Results at $\Delta P = 10$ cm $H_2O$ matched the values obtained by extrapolating agarose permeability data of Johnson and Deen (1996) to zero pressure drop (data not shown). To determine whether the hydrostatic pressure used in these experiments actually compacted the gels and hence produced erroneous results, permeability was measured at two different pressures (10 cm and 5 cm $H_2O$). The ratio of the two flow rates was 2.37$\pm$0.86 ($N = 12$), approximately equal to the expected value of 2, suggesting that compaction was not significant.

### Visualization by laser scanning microscopy using either confocal reflectance or second harmonic generation

Samples were prepared as described in Transwell inserts and sealed under a coverslip. Confocal reflectance microscopy was performed using a modified Bio-Rad MRC600 (Bio-Rad Laboratories, Hercules, CA), an Olympus 100$\times$ 1.4 NA objective (Olympus America Inc., Melville, NY), and 488 nm light from a Kr-Ar laser (American Laser Corp., Salt Lake City, UT). Reflected light from the back surfaces of the objective was attenuated using a quarter wave plate and an analyzer at the detector (Cheng and Summers, 1990; Friedl et al., 1997; Brightman et al., 2001). Gels were also imaged using second harmonic generation (Williams et al., 2001); 810 nm laser light from a mode-locked Ti:Sapphire was scanned through a sample using a modified Bio-Rad MRC600, and second harmonic light was collected using a 405DF33 bandpass filter and an HC125-02 photomultiplier tube (Hammamatsu, Bridgewater, NJ).
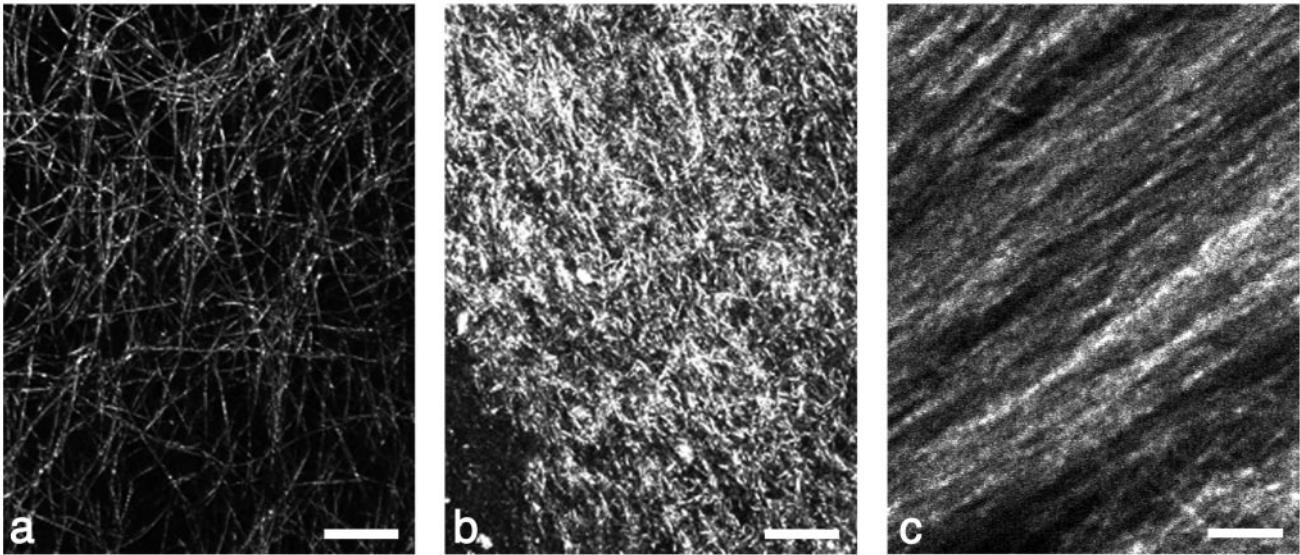
FIGURE 1   (*a* and *b*) Confocal reflectance microscopy of 0.24% (*a*) and 4.5% (*b*) collagen gels. Note the long collagen fibers in *a* in comparison to the shorter collagen fibers in *b* (bar = 10 $\mu$m). (*c*) Second harmonic image of 0.04% collagen gel subsequently centrifuged to high concentration. Note the retention of long fibers as in (*a*) (bar = 10 $\mu$m).

## Theoretical models

### Effective medium model

To account for hydrodynamic interactions and relate the permeability of a matrix to its diffusive hindrance, Phillips et al. (1989) proposed the Brinkman (or effective medium) model for a stationary sphere in imposed flow. This model was later modified slightly to account for hindered diffusion in a medium of interest (Solomentsev and Anderson, 1996; Phillips, 2000):

$$\frac{D}{D_0} = \frac{\alpha}{\left\{1 + \left(\frac{R_h^2}{K}\right)^{1/2} + \frac{1}{9}\left(\frac{R_h^2}{K}\right)\right\}}$$

The model relates $D$ and $K$ in an immobile, rigid, and homogeneous medium under the assumption that the ratio of a molecule's diffusion coefficient in the medium and solution ($D/D_0$) is related to its partition coefficient between the phases. The factor $\alpha$ is a constant of proportionality introduced to improve the quality of curve fits to this equation. The effective medium model, when used in combination with the Carman-Kozeny model (Carman, 1937) below, was found by Pluen et al. (1999) to give the best correlation with pore size in agarose gel experiments.

### Carman-Kozeny model

We estimated pore size in gels using the Carman-Kozeny model to relate permeability, $K$, and pore size, $a$, for a gel of porosity $\varepsilon$:

$$K = \frac{\varepsilon a^2}{4k}$$

This model treats the gel as an array of cylinders characterized by a geometric factor, $k$. If the cylinders are assumed to be randomly oriented in three dimensions, the geometric factor is given by:

$$k = (2k_+ + k_\parallel)$$

where:

$$k_\parallel = \frac{2\varepsilon^3}{(1 - \varepsilon)\left[2\ln\left(\frac{1}{1 - \varepsilon}\right) - 3 + 4(1 - \varepsilon) - (1 - \varepsilon)^2\right]}$$

$$k_+ = \frac{2\varepsilon^3}{(1 - \varepsilon)\left[\ln\left(\frac{1}{1 - \varepsilon}\right) - \frac{1 - (1 - \varepsilon)^2}{1 + (1 - \varepsilon)^2}\right]}.$$

The porosity of the gel is related to the volume fraction, $\phi$, of collagen by the equation $\varepsilon = 1 - \phi$, where $\phi$ is the product of the collagen concentration and the effective specific volume of collagen (protein + bound water), previously reported as 1.89 ml/g (Levick, 1987).

## RESULTS

### Visualization of collagen gels revealed varying degrees of three-dimensional fibrillar assembly

The organization of gels was visualized using a laser-scanning microscope (in confocal reflectance or 2HG mode). Confocal reflectance microscopy and second harmonic generation are both performed in unfixed, hydrated samples, and are useful techniques for the visualization of the collagen network with a spatial resolution of ~0.5 $\mu$m, including distribution and bulk organization of fibers (Friedl et al., 1997; Williams et al., 2001). No structure was detected in collagen solutions at 12–17°C (data not shown). Fig. 1 shows the isotropic, three-dimensional nature of collagen gels of concentrations 0.24% and 4.5%. After gelation, low-concentration gels (0.24%, Fig. 1 *a*) show a highly fibrillar organization as seen previously in gels of compa-

rable concentration (Friedl et al., 1997; Brightman et al., 2001). Unlike the long fibers oriented primarily in two dimensions seen by Friedl et al. (1997), our gels show more 3-dimensionally oriented fibers. At higher collagen concentrations studied (1, 3, 4.5%, Fig. 1 *b*), CLSM revealed poorly organized collagen with denser arrays of shorter fibers replacing the long fibers seen at lower concentrations. Inhomogeneous organization of collagen gels prepared from high-concentration solutions was also seen by transmission electron microscopy (data not shown) as dense, short-banded structures alongside unbanded filamentous structures. These observations agree with previous reports that at concentrations higher than 0.5%, collagen gels in vitro are formed of a mixture of banded fibrils and filamentous structures (Williams et al., 1978). All these gels had an apparent pore size roughly equal to or greater than the ~0.5 $\mu$m spatial resolution of the microscope.

When low-concentration collagen solutions were gelated and <u>then</u> centrifuged to a higher concentration, a dense mat of highly fibrillar collagen was formed (Fig. 1 *c*) with many long fibers compressed close together, with an interfibrillar spacing close to or smaller than the ~0.5 $\mu$m resolution of the microscope. Note that the presence of organized structures does not preclude the existence of unpolymerized collagen in what appear to be void spaces.

## Collagen gels significantly hinder molecular diffusion

Diffusion data obtained in collagen gels prepared from solutions of various concentrations are shown in Fig. 2 *a*, along with data for diffusion in saline and in HA solution. Results of a one-sample *t*-test on slopes of diffusion coefficient versus collagen concentration for representative tracer molecules (dextran 4K, BSA, dextran 2M) verified that the diffusion coefficients decrease significantly ($p < 0.05$) with increasing collagen content. The hydrodynamic radius, $R_h$, of each molecule was determined from its diffusion coefficient in solution, $D_0$, and the Stokes-Einstein relation, under the assumption that the molecule assumes a spherical configuration:

$$D_0 = \frac{k_B T}{6 \pi \mu R_h}$$

where $k_B$ is Boltzmann's constant, $k_B = 1.38 \times 10^{-23}$ J/deg; $T$ is temperature in K, and $\mu$ is the viscosity of water.

For reference, correction to 37°C of the diffusion data of Shenoy and Rosenblatt (1995) in 30 mg/ml succinylated collagen solution yields comparable results with $D_{37°C} = 2.2 \times 10^{-7}$ cm²/s for BSA ($R_h = 4$ nm), and $D_{37°C} = 2.0 \times 10^{-7}$/s cm²/s for 69 kD dextran ($R_h = 6$ nm). The linearity of the data sets indicates that the different classes of tracer particles (globular proteins, dextrans, liposomes) behave similarly in our experiments, so that particle conformation
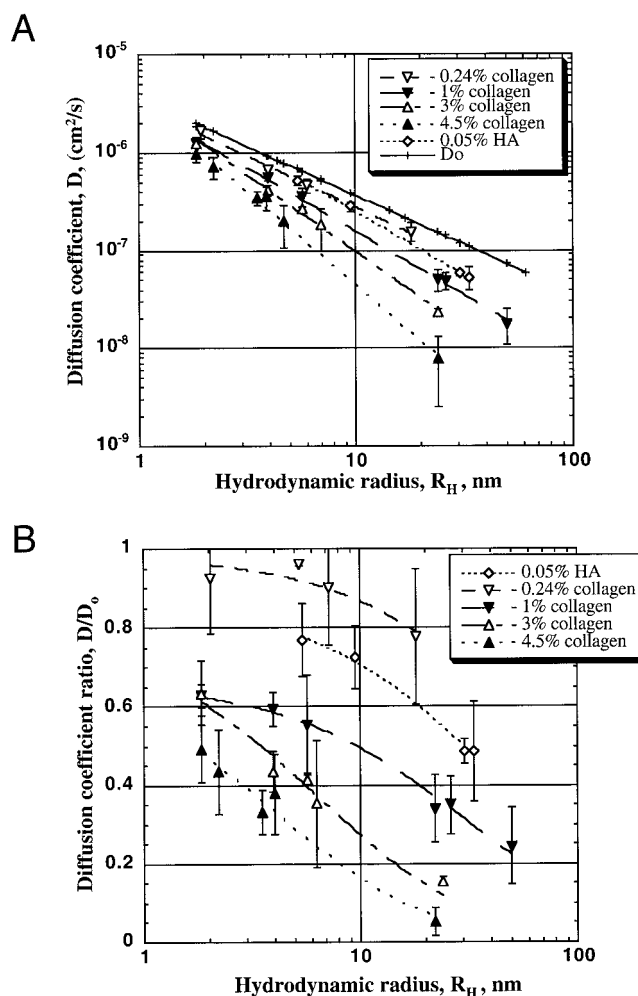


FIGURE 2 FRAP data for diffusion coefficients of tracer molecules at 37°C in saline, 0.4% HA, and 0.24, 1, 3, and 4.5% collagen gels. (*a*) Diffusion coefficients (*D*) as a function of tracer molecule hydrodynamic radius ($R_h$). Lines represent linear fits to data. (*b*) Diffusional hindrance ($D/D_0$, where $D_0$ is diffusion coefficient in saline) as a function of tracer molecule hydrodynamic radius. Dotted lines represent least-square-error fits to effective medium model (mean ± SD).

and interaction with the matrix do not introduce experimental confounds. In Fig. 2 *b* we plot the ratio of the diffusion coefficients obtained in gels to those in free solution as a function of the experimental hydrodynamic radius, to more clearly illustrate the hindrance presented by the gels. The data clearly indicate that at physiologically relevant concentrations (1–4.5%), collagen poses a significant barrier to diffusive transport. HA solutions at 0.05% (0.5 mg/ml) showed statistically significantly less diffusive hindrance relative to the >1% collagen physiological gels studied here ($p < 0.001$ for BSA). This HA concentration used was chosen to correspond to the HA content of the four tumors under consideration (see below). At much higher HA concentrations (0.4%), we found significant diffusive hindrance ($D/D_0 \sim 0.56 \pm 0.11$ for IgG, $D/D_0 \sim 0.27 \pm 0.04$ for 2M MW

**TABLE 1** **Interstitial matrix composition of human and murine tumors grown in mouse dorsal chambers (based on data of Netti *et al.,* 2000)**

| Tumor Type | Collagen Content (mg/g wet tissue) | HA Content (mg/g wet tissue) | IM Collagen (mg/ml IM) | IM HA (mg/ml IM) |
|---|---|---|---|---|
| MCaIV | 1.8 ± 0.5 | 0.16 ± 0.03 | 9.0 ± 2.5 | 0.80 ± 0.15 |
| LS174T | 1.8 ± 0.5 | 0.11 ± 0.02 | 9.0 ± 2.5 | 0.55 ± 0.10 |
| U87 | 8.9 ± 4.2 | 0.11 ± 0.03 | 44.5 ± 21 | 0.55 ± 0.15 |
| HSTS26T | 5.8 ± 1.1 | 0.16 ± 0.02 | 29 ± 5.5 | 0.80 ± 0.10 |

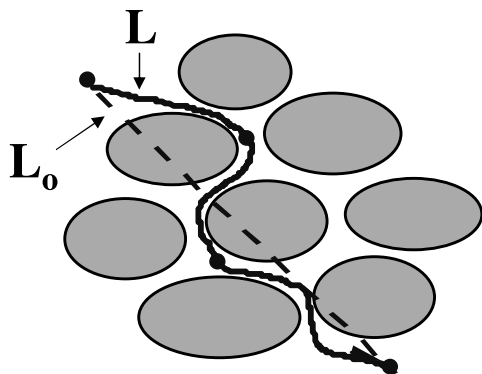Dextran), equivalent to that found in previous studies (De Smedt et al., 1994) (data not shown).

## Diffusion data in gels closely match previous measurements in tumors

We studied gels prepared from 1% (10 mg/ml), 3% (30 mg/ml), and 4.5% (45 mg/ml) solutions specifically to allow comparison with diffusion data obtained by Netti et al. (2000) and Pluen et al. (2001) in the following tumors implanted in mouse dorsal chambers: human colon adenocarcinoma LS174T, mammary carcinoma MCaIV, human soft tissue sarcoma HSTS-26T, and human glioblastoma U87. Measurements by Netti et al. of collagen and HA content in tumors are given in Table 1. IM concentrations in these tumors are estimated by approximating the interstitial volume fraction of the tumor as $f_v = 0.20$ (Jain, 1987) and assuming that (1) matrix components are distributed throughout the interstitial volume, and (2) tissue density is ~1 g/ml. Although the interstitial volume fraction will vary between tumors, reaching up to 50% (unpublished data) and matrix component distribution is not uniform within a given tumor, these approximations provide a rough basis for comparison.

To compare diffusion in gels and tumors, we also account for the tortuosity of the interstitial space resulting from cellular obstacles, as illustrated in Fig. 3. Diffusion along an interstitial path with tortuosity $\tau$ is reduced according to $D_{IM} = D_{gel}/\tau^2$ (Nicholson and Phillips, 1981; Nicholson and Sykova, 1998). Tortuosity is difficult to measure and exhibits inter and intratumor variation. In the absence of detailed data on the tortuosity of the tumor types in question, the tortuosity of a well-packed system of cells can be estimated theoretically, although such a theoretical estimate is a possible source of error. Analytical and numerical calculations have yielded the value $\tau = 2^{1/2}$ for two-dimensional diffusion in arrays of cells with negligible intercellular spacing, and for diffusion in a two-dimensional isotropic pore network (Blum et al., 1989; Chen and Nicholson, 2000). We use this value to adjust gel data for comparison with tumor tissue data, because the FRAP technique measures two-dimensional radial diffusion.

In Fig. 4 *a–c*, we compare the adjusted gel diffusion coefficients to the data of Pluen et al. (2001) in tumors of comparable collagen content. Overall, the gel and tumor data match well, especially considering the absence of other matrix components in the gel and the likely differences in collagen organization and distribution between tumors and gels. The absence of other matrix components may explain the faster decrease of $D$ with $R_h$ in tumors than in gels. The difference in slopes is reflected in Fig. 4*d*, which shows an increase in the effective tortuosity, $\tau^* = \sqrt{D_{IM}/D_{gel}}$ with particle size. The effective tortuosity, $\tau^*$, is the value of the tortuosity necessary to completely account for the difference between the gel and tumor diffusion coefficients, and reflects effects beyond the geometric considerations discussed above.

## Gelation of a collagen solution does not significantly affect its diffusional hindrance

Diffusion coefficients were measured in collagen samples pre and postgelation. Measurements were obtained pregelation at 12–17°C and corrected to 37°C using the Stokes-Einstein equation. Confocal reflectance images of collagen solutions verified a lack of observable structure in pregelation samples (figure not shown), which was further confirmed by optical density measurements, which were equivalent to those obtained in water. Pre and postgelation diffusion coefficients were determined for collagen concen-



FIGURE 3 Schematic of the tortuous path encountered by molecules diffusing in the interstitial matrix between tumor cells. Tortuosity is defined as the ratio of effective path length to linear path length ($L/L_o$).

FIGURE 4 (*a–c*) Comparison of tortuosity-corrected diffusion data in gels to diffusion data in tumors from Netti et al., 2000 and Pluen et al., 2001. Corrected diffusion coefficient is calculated as $D/\tau^2$, using estimate $\tau = \sqrt{2}$. Comparisons are show between: 1% gels (○) and data for LS174T, MCAIV, and U87cw (●) (*a*); 3% gels (◇) and HSTS26T (◆) (*b*); and 4.5% gels (△) and U87dc (▲) (*c*). (*d*) Effective tortuosity necessary to account for discrepancy between uncorrected gel data ($D_{gel}$) and tumor data ($D_{IM}$) as a function of tracer molecule hydrodynamic radius. Values are calculated as $\tau = (D_{gel}/D_{IM})^{1/2}$ from linear fits of $D_{gel}$ (Fig. 2 *a*) and $D_{IM}$ (Fig. 5, *a–c*) data.
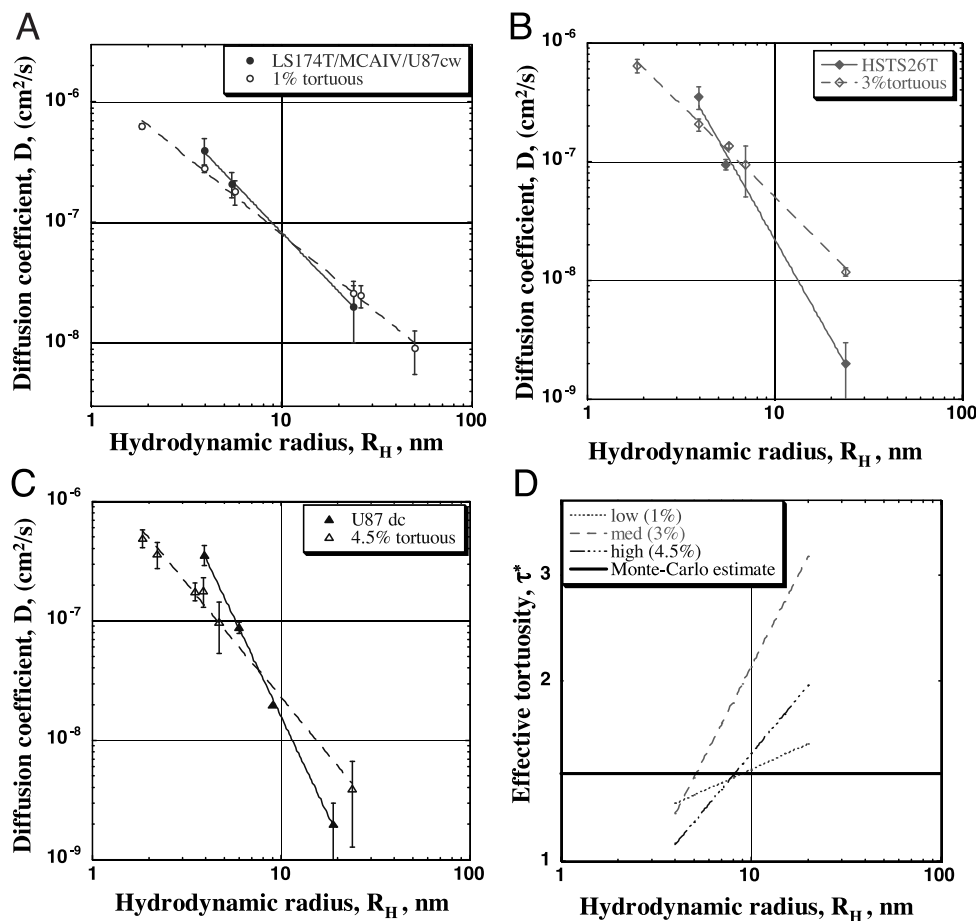


trations of $0–4.5\%$, from multiple measurements within the same sample pre and postgelation, and are shown in Fig. 5. No significant difference was detected between diffusion coefficients pre and postgelation at any of the concentrations of collagen studied, after correction for temperature and viscosity using the Stokes-Einstein relation.

## Diffusion in gels prepared by centrifuging low-concentration gels does not match diffusion in gels prepared directly from high-concentration solutions

The diffusion coefficient of 2M MW dextran was measured in $\sim 20\%$ collagen gels prepared by centrifuging previously polymerized $0.04\%$ gels. The measured value of $4.72 \pm 1.7 \times 10^{-8}$ $cm^2$ $s^{-1}$ was significantly faster ($p < 0.01$) than the value of $7.8 \pm 5.3 \times 10^{-9}$ $cm^2$ $s^{-1}$ measured in collagen gels prepared by direct gelation of $4.5\%$ collagen solutions as discussed above.

## The effective medium model underpredicts the permeability of collagen gels

The Darcy permeability of 1%, 3%, and 4.5% collagen gels was determined experimentally and also estimated from diffusion data using the effective medium model. Curve-fits of the diffusion data to the model are shown in Fig. 2 *b*, and the experimental measurements and model estimates of the Darcy permeability are compared in Fig. 6 *a*. The experimental values and model estimates agree only for the 1% gels. Above this concentration, the experimental measurements are increasingly greater than the model estimates, with an order of magnitude difference for the 4.5% gels. This difference in permeability values translates into a difference in pore size as estimated by the Carman-Kozeny model, as shown in Fig. 6 *b*.

## Measured permeability of gels does not correspond to tumor permeability

The permeability of gels correlated inversely with collagen content, whereas the permeability of tumors with corresponding collagen content did not (Fig. 7 *a*). To compare the permeability measurements in collagen gels with the published measurements in tumors, the gel measurements must be adjusted by the area fraction ($f_A$) in a tumor slice and the tortuosity, or increased length of the fluid path through the slice. Adjusting the gel data by $K_{tumor} = K_{gel} f_A/\tau$, where the interstitial area fraction is estimated at $f_A = 0.2$ and the theoretical estimate $\tau = 2^{1/2}$ is used for the
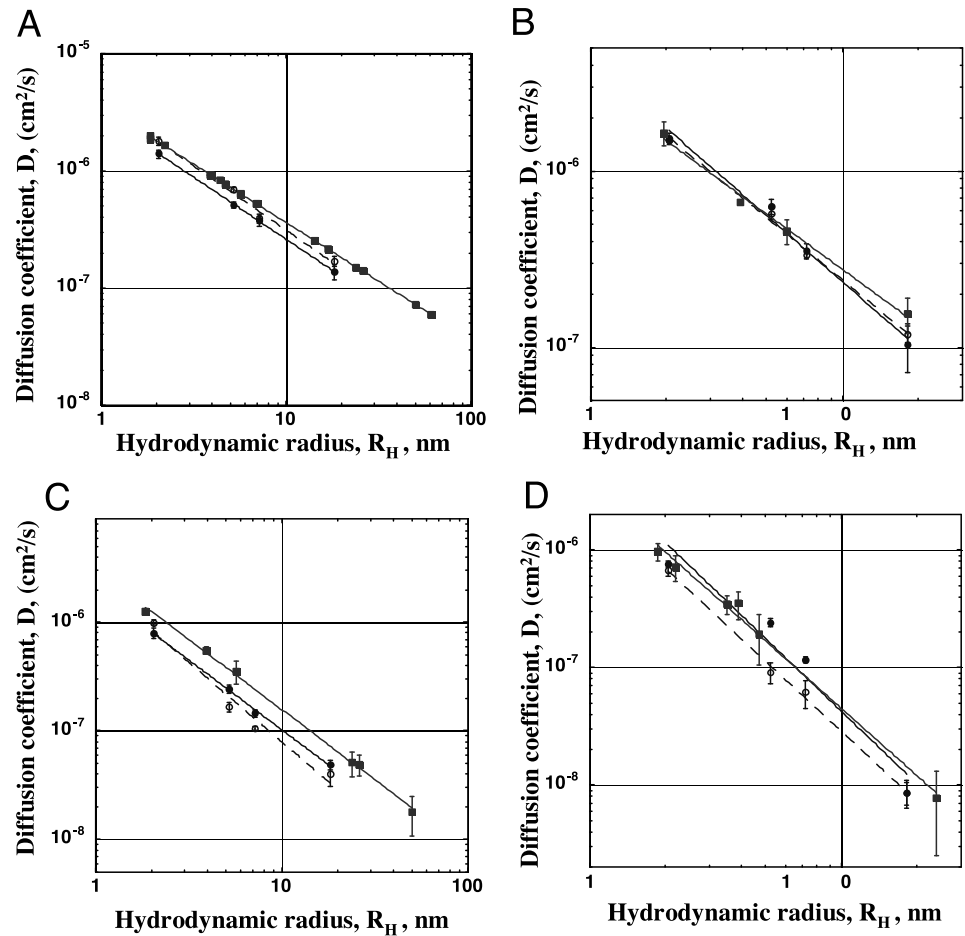
FIGURE 5 Comparison of diffusion data before and after incubation (gelation) at 37°C for free solution (*a*), 0.24% collagen gel (*b*), 1% collagen gel (*c*), and 4.5% collagen gel (*d*). Pre-incubation data (○) obtained at 12–17°C and corrected to 37°C using the Stokes-Einstein equation, and postincubation data (●) obtained at 37°C represent multiple measurements in the same sample. Averaged data (■) obtained from multiple samples and presented earlier in Fig. 2 are provided for reference.

tortuosity, we obtained the data shown in Fig. 7 *b* alongside published tumor measurements. Collagen gels corrected for the absence of cells are significantly less permeable than tumors of comparable collagen content, although direct comparison may be complicated by the use of different permeability measurement techniques for gels and tumors, and by intratumoral ECM heterogeneity.

## DISCUSSION

### Collagen can account for most of the diffusional hindrance measured in tumors studied

Collagen significantly impedes diffusion, and the extent to which it does so, when corrected for the tortuosity of the interstitium, is consistent with diffusion data obtained in tumors of comparable collagen content (Fig. 4 *a–c*). Note that the slope of the diffusion data differs between gel and tumor data sets. This phenomenon is also seen as an increase with molecular size of the effective tortuosity in tissue (Fig. 4 *d*), and has been observed in studies of diffusion in the brain (Nicholson and Sykova, 1998). In tumors, matrix components other than collagen could affect this slope by differentially affecting the diffusion of small

versus large molecules. Heterogeneity of collagen structure and distribution in tumors, as shown by Pluen et al. (2001) may also differentially affect particles of different sizes. Thus the effective tortuosity in a tumor scales with particle size and is heterogeneous, depending on the local tissue composition and structure.

Our results suggest that diffusion in pure collagen gels mimics that in the tumor IM over the wide range of particle sizes studied. However, extrapolating these results to particles with a hydrodynamic radius larger than 2M MW dextrans may not be justified. The Carman-Kozeny estimates of pore size and the linearity of the diffusion data sets suggest that the particles we used are smaller than the effective pore sizes of the gels studied. As particle sizes approach the effective pore size of the media, the fine structure of the matrix is expected to critically influence transport hindrance, and in vitro gels may no longer capture the in vivo behavior. Rusakov and Kullmann (1998) argued that large molecules comparable to the pore size experience greater hindrance due to viscous interactions unaccounted for in tortuosity corrections. Matrix pore size is expected to be different in gels than in tumors, where factors such as compaction of collagen fibrils by fibroblasts (Friedl et al.,
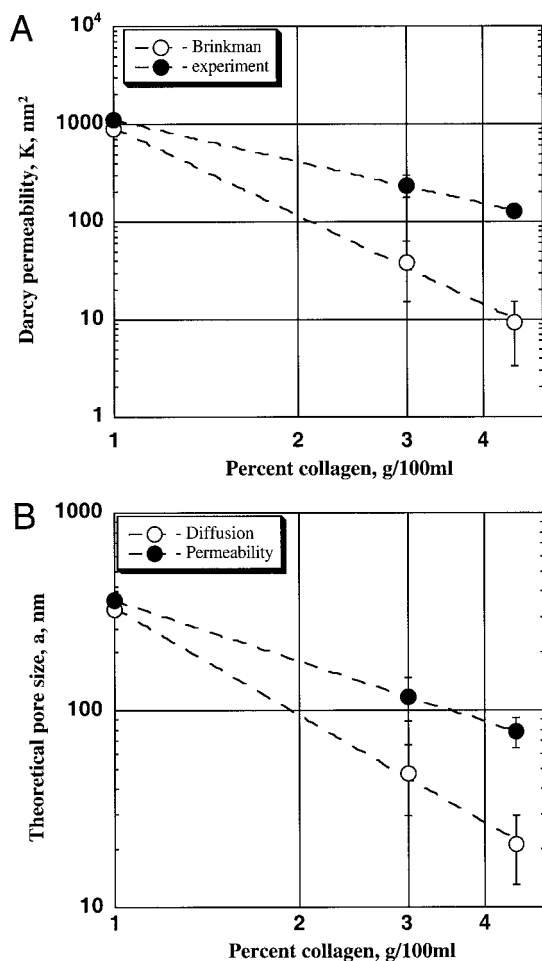
FIGURE 6 (a) Comparison of experimental measurements (●) and model-based predictions (○) of Darcy permeability as a function of collagen gel concentration. Model predictions are obtained from application of the effective medium model to diffusion data (see curve fits, Fig. 2 b). (b) Comparison of theoretical pore size predicted by Carman-Kozeny model from experimental measurements of Darcy permeability (●), and from effective medium estimates of permeability from diffusion data (○).

1997; Guidry and Grinnell, 1987; Huang-Lee et al., 1994) and additional IM molecules such as decorin (Pins et al., 1997) play a role. Thus, although the agreement between the gel and tumor measurements is surprisingly good, these results should not be extrapolated to larger particle sizes.

## Unassembled collagen is implicated in the diffusive hindrance of pure collagen gels

After correction for the effect of temperature on viscosity and molecular motion, there was no significant difference in diffusion between collagen solutions and collagen gels gelated from equivalent concentrations. These data are consistent with those of Shenoy and Rosenblatt (1995), where solutions of succinylated collagen at room temperature were capable of significantly slowing diffusion. This fact, combined with imaged pore sizes that appear too large (several hundreds of nanometers) to significantly hinder diffusion, suggests that unassembled collagen in the void spaces of these gels plays a role in hindering diffusion.

Note that gels formed by gelation of different concentrations of collagen are not simply more or less concentrated versions of the same structure. The highly fibrillar network formed from the gelation of low-concentration collagen solutions is qualitatively different from the dense array of short fibers and partially formed structures generated upon gelation of high-concentration collagen solutions. When gels formed from low-concentration collagen solutions (~0.04%) are subsequently centrifuged to higher concentrations (~20%) than the gels formed by direct gelation of high-concentration solutions (~4.5%), the resultant gel retains its original highly fibrillar structure, but the long fibers are significantly compacted, forming a dense mat. Not surprisingly, these qualitatively different gels prepared by centrifugation postgelation do not reproduce the diffusive hindrance of gels prepared by simple gelation, exhibiting a significantly higher diffusion coefficient for 2M MW dextran. The compaction of the array of long fibers initially formed at low concentrations could be markedly inferior to that of the dense array of short fibers and partially formed structures generated by gelating a high-concentration solution. Additionally, it is known that the partitioning of collagen between assembled and unassembled states varies with the concentration at which the gel is polymerized (Williams et al., 1978). We conclude that the poorly assembled gels formed by simple polymerization of collagen solutions and containing that proportion of unassembled collagen dictated by the concentration at time of gelation are the gels that quantitatively mimic the diffusive hindrance of tumor interstitium of equivalent collagen concentration.

Although these gels quantitatively mimic the diffusive hindrance of the tumor interstitium, this does not mean that these gels completely reproduce the interstitial matrix at a molecular level. Other matrix molecules are certainly present in vivo, and the structure of collagen assembled in vivo is likely to differ from that assembled in vitro. However, the poorly assembled gels studied here do have structural similarities to the collagen of the tumor interstitium, which is poorly organized in comparison to normal tissue. Pluen et al. (2001) reported that subcutaneous U87 tumors stain positively for collagen type I in the tumor center where only few fibrils were detected by EM visualization, whereas the periphery of U87 and other tumor types showed a high density of collagen fibrils. These results suggest that unassembled molecules between the fibers of the interstitial matrix can influence the diffusion of macromolecules in vivo just as they seem to do in vitro. In pure collagen type I gels, these unassembled molecules can only be collagen type I, while in vivo, these unassembled molecules may include other matrix molecules, such as nonfibrillar collagen type I, other collagen types, or HA.
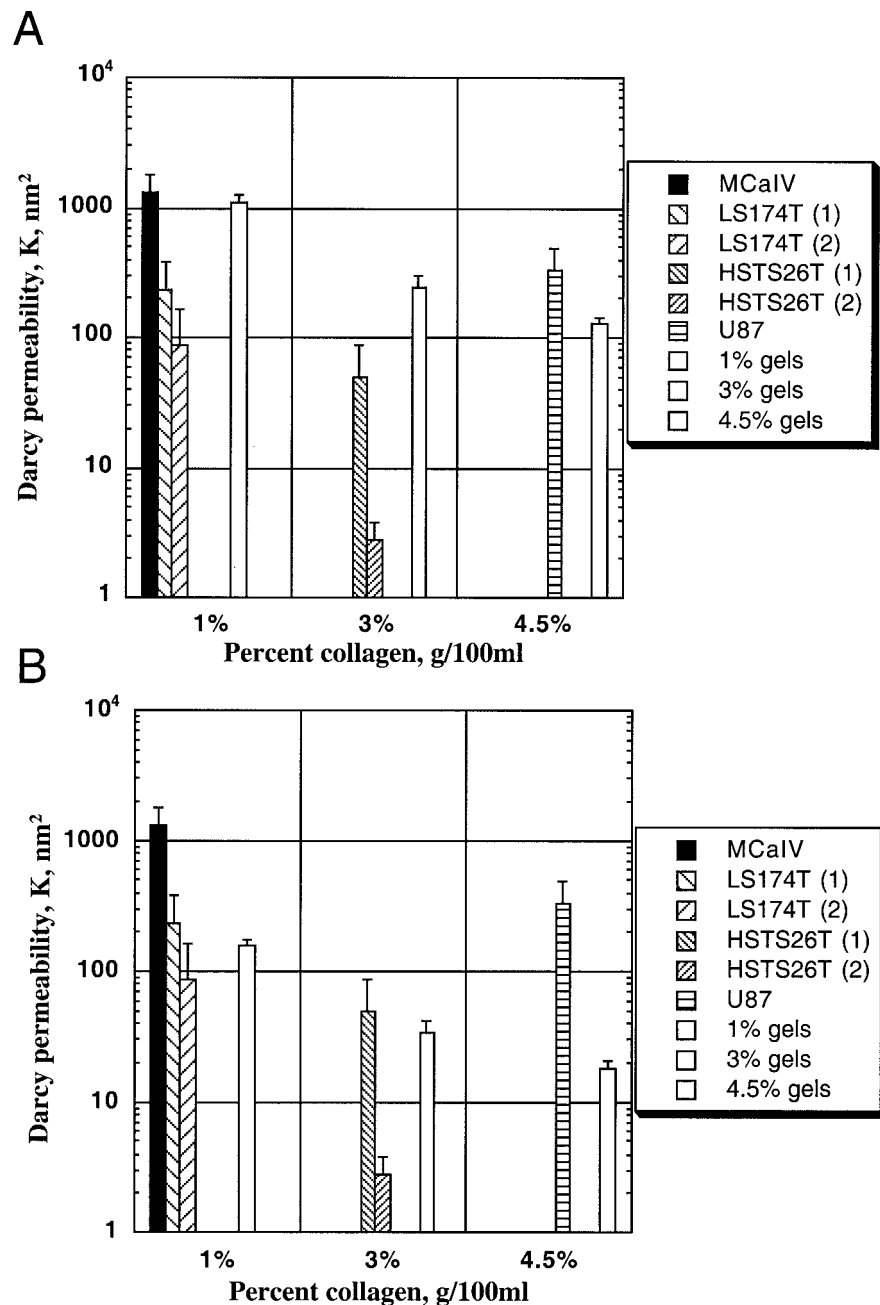
## A



## B



FIGURE 7 (*a*) Comparison of Darcy permeability measurements in tumors and gels of measured collagen concentrations. Confined compression measurements of *K* in MCaIV, LS174T (1), HSTS26T (1), and U87 tumors (Netti et al., 2000), micropipette measurements of *K* in LS174T (2) tumors (Boucher et al., 1998), and pressure gradients across clamped HSTS26T (2) tumor tissue sections (Griffon-Etienne et al., 1999). (*b*) Comparison of Darcy permeability measured in tumors to those in gels when corrected for area fraction and tortuosity.

## At concentrations relevant to the tumors studied, pure collagen is a major diffusive barrier and offers more hindrance than pure hyaluronan

The diffusion data attest to the ability of collagen gels at concentrations comparable to those of the tumor IM to significantly hinder diffusive transport (Fig. 2). In contrast, HA solutions at concentrations comparable to the tumors analyzed here (0.05%) pose a weaker barrier to diffusion. For 3% and 4.5% collagen gels, the diffusive barrier offered by HA (i.e., $D/D_0$) is far less than that offered by collagen, suggesting that in tumors with these collagen concentrations (e.g., HSTS26T and U87), collagen alone can account for

the diffusive hindrance in the tumor. For the lowest collagen concentration gels (1%), the barrier offered by HA is over half the barrier offered by collagen, suggesting that in tumors with this collagen concentration (e.g., LS174T) HA may have some influence on diffusive hindrance.

This finding does not apply to tissues with higher HA content, including the tumor spheroids studied by Davies et al. (2002) and other GAG-rich tissues, such as cartilage. Furthermore, the pure HA solutions do not replicate possible in vivo interactions between different species of matrix molecules (e.g., Turley et al., 1985), which may affect transport properties.

## Collagen gels studied here pose a greater diffusive than hydraulic barrier

Data collected from several organs have indicated that permeability is inversely correlated to collagen content (Levick, 1987). We have found the same trend in collagen gels. However, the permeability values in tumors did not match the data in collagen gels quantitatively, nor did they show the qualitative inverse correlation with collagen content. Furthermore, when the data for collagen gels were adjusted for area fraction and tortuosity in tumors, the permeability was higher in tumors than in gels of comparable concentration. The differences in permeability could be due partially to measurement techniques. Even within tumors, the confined compression technique used by Netti et al. (2000) predicted significantly higher hydraulic conductivity compared to the micropipette approach (Boucher et al., 1998) and clamp methods (Griffon-Etienne et al., 1999). The lack of correlation between collagen and permeability observed by Netti et al. in tumors suggests a more important contribution from other matrix molecules.

Estimates of gel permeability based on the effective medium model matched experimental measurements of permeability only for 1% collagen gels (Fig. 6). At greater concentrations, the diffusion-based effective medium model values increasingly underestimated the true permeability. In contrast, the model was reported to be accurate for agarose gels (Pluen et al., 1999), and underestimated *diffusion coefficients* in various other gels, a deviation qualitatively opposite to that observed here (Phillips, 2000). In general, discrepancies between gel measurements and effective medium model predictions may result from model assumptions of fiber rigidity, immobility, and homogeneity. Furthermore, the effective medium model empirically relates two fundamentally different modes of transport (convection and diffusion), which can be differentially regulated. The accuracy of the effective medium prediction at low collagen concentration and the increasing discrepancy at higher collagen concentrations may also indicate that high concentrations of poorly organized collagen pose a greater barrier to diffusion than to convection. This argument is also supported by the observation that diffusional hindrance in tumors correlates with collagen content (Pluen et al., 2001), whereas the measured permeability of tumors does not (Netti et al., 2000).

## CONCLUSIONS

In conclusion, our data show that collagen at physiological concentrations presents a major barrier to molecular diffusion, especially for larger particles. Furthermore, theoretical correction of gel diffusion data for the effects of in vivo tortuosity yielded good agreement with in vivo measurements in tumors of comparable collagen concentration. The diffusive hindrance data combined with imaging of the gels and permeability measurements suggest that unassembled collagen in the void spaces of the gel plays a role in hindering diffusion. In vivo, this role may be played by unassembled collagen or other matrix molecules. These findings support our hypothesis that collagen is a major contributor to diffusive hindrance in tumors. In addition, it suggests that in vitro gel models can be used to investigate diffusion in tissues, with theoretical correction for issues such as tortuosity providing the necessary bridge between the in vivo and in vitro measurements. This work has important implications for drug delivery in tumors and for tissue engineering, where transport in collagen-based tissue replacements or scaffolds is an important design consideration. Furthermore, interfering with collagen synthesis or reducing collagen content may improve drug delivery to tumors (McKee et al., 2001).

## REFERENCES

Alberts, B., D. Bray, J. Lewis, M. Raff, K. Roberts, and J. Watson. 1994. Extracellular Matrix of Animals. *In* Molecular Biology of the Cell, 3rd Ed. Garland Publishing, New York, 971–995.

Berk, D. A., F. Yuan, M. Leunig, and R. K. Jain. 1993. Fluorescence photobleaching with spatial Fourier analysis: measurement of diffusion in light-scattering media. *Biophys. J.* 62:2428–2436.

Berk, D. A., F. Yuan, M. Leunig, and R. K. Jain. 1997. Direct in vivo measurement of targeted binding in a human tumor xenograft. *Proc. Natl. Acad. Sci. USA.* 95:1785–1790.

Blum, J. J., G. Lawler, M. Reed, and I. Shin. 1989. Effect of cytoskeletal geometry on intracellular diffusion. *Biophys. J.* 56:995–1005.

Boucher, Y., C. Brekken, P. A. Netti, L. T. Baxter, and R. K. Jain. 1998. Intratumoral infusion of fluid: estimation of hydraulic conductivity and implications for the delivery of therapeutic agents. *Br. J. Cancer.* 78:1442–1448.

Brightman, A. O., B. P. Rajwa, J. E. Sturgis, M. E. McCallister, J. P. Robinson, and S. L. Voytik-Harbin. 2001. Time-lapse confocal reflection microscopy of collagen fibrillogenesis and extracellular matrix assembly in vitro. *Biopolymers.* 54:222–234.

Carman, P. C. 1937. Fluid flow through granular beds. *Trans. Inst. Chem. Eng.* 15:150–166.

Chang, Y. S., L. L. Munn, M. V. Hillsley, R. O. Dull, J. Yuan, S. Lakshminarayanan, T. W. Gardner, R. K. Jain, and J. M. Tarbell. 2000. Effect of vascular endothelial growth factor on cultured endothelial cell monolayer transport properties. *Microvasc. Res.* 59:265–277.

Chen, K. C., and C. Nicholson. 2000. Changes in brain cell shape create residual extracellular space volume and explain tortuosity behavior during osmotic challenge. *Proc. Natl. Acad. Sci. USA.* 97:8306–8311.

Cheng, P. C., and R. G. Summers. 1990. Image contrast in confocal microscopy. *In* Handbook of Biological Confocal Microscopy. J. B. Pawley, editor. Plenum Press, New York, 170–196.

Costantini, L. C., J. C. Bakowska, X. O. Breakefield, and O. Issacson. 2000. Gene therapy in the CNS. *Gene Ther.* 7:93–109.

Davies, C. de L., D. Berk, A. Pluen, and R. K. Jain. 2002. Comparison of IgG diffusion and extracellular matrix composition in rhabdomyosarcomas grown in mice versus in vitro as spheroids reveals the role of host stromal cells. *Br. J. Cancer.* 86:1639–1644.

De Smedt, S. C., A. Lauwers, J. Demeester, Y. Engelborghs, G. De Mey, and M. Du. 1994. Structural information on hyaluronic acid solutions as studied by probe diffusion experiments. *Macromolecules.* 27:141–146.

Friedl, P., K. Maaser, C. E. Klein, B. Niggemann, G. Krohne, and K. S. Zanker. 1997. Migration of highly aggressive MV3 melanoma cells in 3-dimensional collagen lattices results in local matrix reorganization and shedding of $\alpha$2 and $\beta$1 integrins and CD44. *Cancer Res.* 57:2061–2070.

Gabizon, A., D. Goren, R. Cohen, and Y. Barenholz. 1998. Development of liposomal anthracyclines: from basics to clinical applications. *J. Controlled Release.* 53:275–279.

Gribbon, P. M., A. Maroudas, K. H. Parker, and C. P. Winlove. 1998. Water and solute transport in the extracellular matrix: physical principles and macromolecular determinants. *In* Connective Tissue Biology: Integration and Reductionism. R. K. Reed and K. Rubin, editors. Portland, London. 95–124.

Griffon-Etienne, G., Y. Boucher, C. Brekken, H. D. Suit, and R. K. Jain. 1999. Taxane-induced apoptosis decompresses blood vessels and lowers interstitial fluid pressure in solid tumors: clinical implications. *Cancer Res.* 59:3776–3782.

Guidry, C., and F. Grinnell. 1987. Heparin modulates the organization of hydrated collagen gels and inhibits gel contraction by fibroblasts. *J. Cell Biol.* 104:1097–1103.

Huang-Lee, L. L. H., J. H. Wu, and M. E. Nimni. 1994. Effects of hyaluronan on collagen fibrillar matrix contraction by fibroblasts. *J. Biomed. Mater. Res.* 28:123–132.

Jain, R. K. 1987. Transport of molecules in the tumor interstitium: a review. *Cancer Res.* 47:3039–3051.

Jain, R. K. 1998. The next frontier of molecular medicine: delivery of therapeutics. *Nature Med.* 4:655–657.

Jain, R. K. 1999. Transport of molecules, particles and cells in solid tumors. *Annu. Rev. Biomed. Eng.* 1:241–263.

Johnson, E. M., and W. M. Deen. 1996. Hydraulic permeability of agarose gels. *AIChE J.* 42:1220–1224.

Kulkarni, S. B., G. V. Betageri, and M. Singh. 1995. Factors affecting microencapsulation of drugs into liposomes. *J. Microencapsul.* 12: 229–246.

Levick, J. R. 1987. Flow through interstitium and other fibrous matrices. *Q. J. Exp. Physiol.* 72:409–438.

McKee, T. D., A. Pluen, Y. Boucher, S. Ramanujan, E. N. Unemori, B. Seed, and R. K. Jain. 2001. Relaxin increases the transport of large molecules in high collagen content tumors. *Proc. Am. Assoc. Cancer Res.* 42:30.

Netti, P. A., D. A. Berk, M. A. Swartz, A. J. Grodzinsky, and R. K. Jain. 2000. Role of extracellular matrix assembly in interstitial transport in solid tumors. *Cancer Res.* 60:2497–2503.

Netti, P. A., L. M. Hamberg, J. W. Babich, D. Kierstead, W. Graham, G. J. Hunter, G. L. Wolf, A. Fischman, Y. Boucher, and R. K. Jain. 1999. Enhancement of fluid filtration across tumor vessels: implication for delivery of macromolecules. *Proc. Natl. Acad. Sci. USA.* 96:3137–3142.

Nicholson, C., and J. M. Phillips. 1981. Ion diffusion modified by tortuosity and volume fraction in the extracellular microenvironment of the rat cerebellum. *J. Physiol.* 321:225–257.

Nicholson, C., and E. Sykova. 1998. Extracellular space structure revealed by diffusion analysis. *Trends Neurosci.* 21:207–215.

Phillips, R.J. 2000. A hydrodynamic model for hindered diffusion of proteins and micelles in hydrogels. *Biophys. J.* 79:3350–3354.

Phillips, R. J., W. M. Deen, and J. F. Brady. 1989. Hindered transport in fibrous membranes and gels. *AIChE J.* 35:1761–1769.

Pins, G. D., D. L. Christiansen, R. Patel, and F. H. Silver. 1997. Self-assembly of collagen fibers. Influence of fibrillar alignment and decorin on mechanical properties. *Biophys. J.* 73:2164–2172.

Pluen, A., Y. Boucher, S. Ramanujan, T. D. McKee, T. Gohongi, E. di Tomaso, E. B. Brown, Y. Izumi, R. B. Campbell, D. A. Berk, and R. K. Jain. 2001. Role of tumor-host interactions in interstitial diffusion of macromolecules: cranial vs. subcutaneous tumors. *Proc. Natl. Acad. Sci. USA.* 98:4628–4633.

Pluen, A., P. A. Netti, R. K. Jain, and D. A. Berk. 1999. Diffusion of macromolecules in agarose gels: comparison of linear and globular configurations. *Biophys. J.* 77:542–552.

Rusakov, D., and D. Kullmann. 1998. Geometric and viscous components of the tortuosity of the extracellular space in the brain. *Proc. Natl. Acad. Sci. USA.* 95:8975–8980.

Sano, A., T. Hojo, M. Maeda, and K. Fujioka. 1998. Protein release from collagen matrices. *Adv. Drug Deliv. Rev.* 31:247–266.

Shenoy, V., and J. Rosenblatt. 1995. Diffusion of macromolecules in collagen and hyaluronic acid, rigid-rod-flexible polymer, composite matrices. *Macromolecules.* 28:8751–8758.

Solomentsev, Y. E., and J. L. Anderson, 1996. Rotation of a sphere in Brinkman fluids. *Phys. Fluids.* 8:1119–1121.

Turley, E. A., C. A. Erickson, and R. P. Tucker. 1985. The retention and ultrastructural appearances of various extracellular matrix molecules incorporated into three-dimensional hydrated collagen lattices. *Dev. Biol.* 109:347–369.

Williams, B. R., R. A. Gelman, D. C. Poppke, and K. A. Piez. 1978. Collagen fibril formation. Optimal in vitro conditions and preliminary kinetic results. *J. Biol. Chem.* 253:6578–6585.

Williams, R. M., W. R. Zipfel, and W. W. Webb. 2001. Multiphoton microscopy in biological research. *Curr. Opin. Chem. Biol.* 5:603–608.